LANGMUIR

pubs.acs.org/Langmuir Article

PDMS-Zwitterionic Hybrid for Facile, Antifouling Microfluidic Device Fabrication

Anthony Mercader, $^{\nabla}$ Sang-Ho Ye, $^{\nabla}$ Seungil Kim, Ryan A. Orizondo, Sung Kwon Cho, and William R. Wagner*



Cite This: Langmuir 2022, 38, 3775-3784



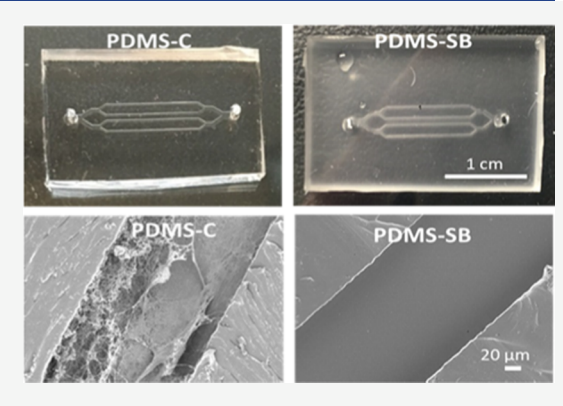
ACCESS I

Metrics & More

Article Recommendations

s Supporting Information

ABSTRACT: Poly(dimethylsiloxane) (PDMS) has been used in a wide range of biomedical devices and medical research due to its biostability, cytocompatibility, gas permeability, and optical properties. Yet, some properties of PDMS create critical limitations, particularly fouling through protein and cell adhesion. In this study, a diallyl-terminated sulfobetaine (SB-diallyl) molecule was synthesized and then directly mixed with a commercial PDMS base (Sylgard 184) and curing agent to produce a zwitterionic group-bearing PDMS (PDMS–SB) hybrid that does not require a complex or an additional surface modification process for the desired end product. In vitro examination of antifouling behavior following exposure to fresh ovine blood showed a significant reduction in platelet deposition for the PDMS–SB hybrid surface compared to that of a PDMS control (p < 0.05, n = 5). The manufacturability via soft lithography using the synthesized polymers was



found to be comparable to that for unmodified PDMS. Bonding via O_2 plasma treatment was confirmed, and the strength was measured and again found to be comparable to the control. PDMS—SB microfluidic devices were successfully fabricated and showed improved blood compatibility that could reduce channel occlusion due to clot formation relative to PDMS control devices. Further, gas (CO_2) transfer through a PDMS—SB hybrid membrane was also tested with a proof-of-concept microchannel device and shown to be comparable to that through the PDMS control.

INTRODUCTION

Poly(dimethylsiloxane) (PDMS) has been applied to a broadening array of applications in the biomedical field, including contact lens, catheters, microfluidic devices for biosensors, bioanalytical devices, organ-on-chips, and other medical implants. The PDMS polymer has several advantages including low toxicity, stability against oxidative stress, optical transparency, and high gas permeability. However, some applications are limited by poor adhesion properties, insufficient bulk mechanical properties, and limited processability. More critically, the PDMS surface can be readily fouled by nonspecific protein adsorption and cell adhesion (e.g., platelets when blood is the contacting fluid or bacterial adhesion) attributed in part to the intrinsic hydrophobicity of the material.

To improve the fouling resistance of PDMS, the majority of efforts have focused on surface modification strategies, including plasma treatments, sol—gel methods, layer by layer deposition, surface segregation, silanization, and grafting to or grafting from the surface using various molecules. ^{1,4} However, physical or simple surface treatments to improve hydrophilicity are often transient. Chemical modifications for covalent bonds are preferable to make a relatively stable surface and provide long-term antifouling properties, though most chemical

modifications are complex and associated with multiple steps, thus presenting challenges for mass production. 1,4

Modifications of blood-contacting surfaces with biocompatible and bioinert zwitterionic groups (e.g., phosphorylcholine (PC), sulfobetaine (SB), or carboxybetaine (CB)) have been demonstrated to be effective at minimizing the fouling of biomaterials by reducing protein adsorption or thrombotic deposition. Some zwitterionic groups were also used for the surface modification of PDMS and exhibited an antifouling ability. However, the performance relies on surface modification techniques, which can be highly complex. Furthermore, the coating stability remains a major concern, as the surface properties of such PDMS modifications could change with time (showing fast hydrophobic recovery after the surface hydrophilization). Thus, the development of an antifouling PDMS polymer bearing zwitterionic groups in the polymer backbone rather than on the surface was considered as

Received: December 17, 2021 Revised: March 8, 2022 Published: March 16, 2022





Scheme 1. (A) Synthesis of a Diallyl-Terminated Sulfobetaine (SB-Diallyl) and (B) the Direct Application to a Commercial PDMS (Sylgard 184) for Conventional Microfluidic Device Fabrication

Langmuir

a preferable solution. Such an approach not only does not require a complex or additional surface modification process for the desired end product but also has the potential to address concerns regarding long-term antifouling stability. This approach would also allow the polymer to be used as a structural material for many devices with no need for surface treatment, and it could be compatible with mass production using conventional fabrication methods.

To develop this type of fouling-resistant PDMS derivative material, a diallyl-terminated sulfobetaine molecule (SB-diallyl) was synthesized to be integrated directly with a commercial PDMS base (Sylgard 184, vinyl-terminated PDMS). The resultant SB-diallyl integrated PDMS (PDMS—SB) hybrid membranes, as well as microfluidic devices fabricated by the common PDMS micro(nano)-fabrication process, were assessed (Scheme 1). The PDMS—SB hybrid was characterized by focusing on blood biocompatibility and microfabrication ability. The gas permeability was also evaluated as an indicator for the utilization of these materials in microfluidic artificial lung devices.

EXPERIMENTAL PART

Materials. Diallylmethylamine (97%), 1,3-propanesultone (98%), and dichloromethane (≥99.8%) were purchased from Sigma-Aldrich (St. Louis, MO) and used as received, without further purification. 1,1,1,3,3,3-Hexafluoro-2-propanol (HFIP) was purchased from Oakwood Chemical (Estill, SC). Sylgard 184 Silicone Elastomer Kit was purchased from Dow Corning Corporation (Midland, MI).

Synthesis of SB-Diallyl and Integration with PDMS. SB-diallyl was synthesized from diallylmethylamine and 1,3-propane-sultone (Scheme 1A). Briefly, the two monomers (DAMA (2.77 g)/PS (3.35 g) = 1:1.1 molar ratio) were dissolved together in dichloromethane (50 mL) under argon injection for 20 min with the flask sealed and the mixture stirred for 48 h at 40 °C. The solvent was then removed using a centrifuge, and the obtained white

precipitate was further washed with ether and dichloromethane (1:1 mixture) and dried under vacuum (yield rate \sim 70%). The chemical structure of SB-diallyl was confirmed by proton nuclear magnetic resonance (1 H NMR, BrukerBiospin Co., Billerica, MA).

The synthesized SB-diallyl was dissolved in HFIP (50 wt %) and then directly mixed with a commercial PDMS base (Sylgard 184, vinyl-terminated PDMS, Dow, Midland, MI) as well as the curing agent at a 10:1 ratio. The mixed solution was placed under vacuum for 30 min and then moved to an oven at 60 °C for 4 h. The mixing ratios of SB-diallyl/PDMS base were determined based on the approximate molar ratio (0.5:1, 1:1, or 2:1). The actual mixing ratios of SB-diallyl were 0.5, 1.0, or 2 wt % vs Sylgard base, and those are denoted as PDMS–SB-1, PDMS–SB-2, and PDMS–SB-3, respectively.

The uniaxial tensile strength and strain of sample films were measured using an MTS Tytron 250 microforce testing workstation after cutting the films into dumbbell-shaped strips ($2 \times 18 \text{ mm}^2$) and immersing in DI water for 15 h.

Characterization of Thrombotic Deposition. In vitro thrombotic deposition on the PDMS-SB and PDMS control (Sylgard 184) was assessed by a simple rocking test⁷ with citrated fresh ovine blood. Whole ovine blood was collected by jugular venipuncture. NIH guidelines for the care and use of laboratory animals were observed, and all animal procedures were approved by the Institutional Animal Care and Use Committee at the University of Pittsburgh. Each test tube (BD Vacutainer, no additive) with a sample was filled with 5 mL of ovine blood and gently rocked for 2 h at 37 °C on a hematology mixer (Fisher Scientific, Pittsburgh, PA). After ovine blood contact, the polymer membrane surfaces were rinsed with Dulbecco's phosphate-buffered saline (DPBS) to remove any nonadherent blood elements. The surface was then observed by scanning electron microscopy (SEM; JSM-6330F, JEOL USA, Inc., Peabody, MA) after fixing the surface adherent platelets and then serially dehydrating with solutions of increasing ethanol content. Deposited platelets on each surface were also quantified by a lactate dehydrogenase (LDH) assay⁸ with an LDH Cytotoxicity Detection Kit (Clontech Laboratories, Inc. Mountain View, CA).

SB-diallyl

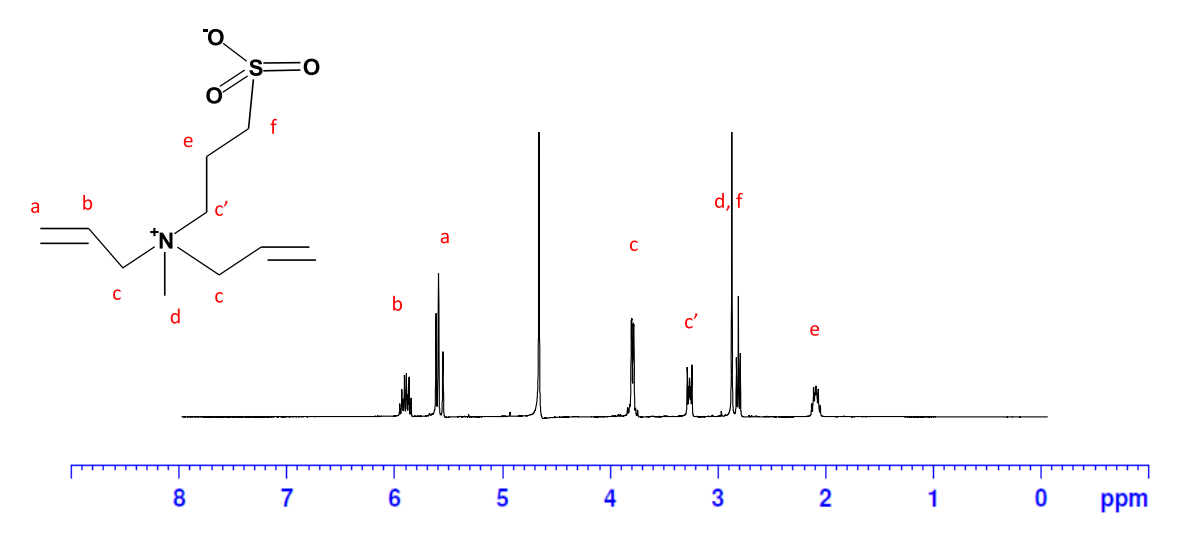


Figure 1. ¹H NMR spectra of SB-diallyl.

In Vitro Hemolysis Assay and Cytotoxicity Testing. Hemocompatibility of the PDMS-SB hybrid was evaluated using fresh ovine blood collected in a sodium citrate tube following the Standard Practice for Assessment of Hemolytic Properties of Materials from the American Society for Testing and Materials (ASTM F756-17).¹⁰ Briefly, the hemoglobin concentration of the whole blood was adjusted to 8 g/dL with DPBS (Ca and Mg free). PDMS-SB samples were washed with 70% EtOH and DPBS in sequence. The washed samples were separately immersed in 5 mL of the whole blood in test tubes, and the tubes were rocked at 37 °C for 3 h. The blood after contact with the sample was centrifuged at 750g for 15 min to collect 1 mL of supernatant. The supernatant was reacted with 1 mL of Drabkin's reagent at 37 °C for 15 min, and its absorbance at 540 nm was recorded. The % hemolysis was calculated from the equation $(A \times 100)/B$, where A = supernatant hemoglobin concentration and B = total hemoglobin concentration in a tube.According to ASTM F756-17, the sample was considered as nonhemolytic if the % hemolysis above the negative control was lower than 2%, slightly hemolytic if between 2 and 5%, and hemolytic if higher than 5%. Nonsample contacted ovine blood was used as a negative control.

The cytotoxicity of PDMS-SB samples was investigated by an indirect test (an elution medium test according to the ISO10993-5 standard) and a Live/Dead assay. 10 Briefly, primary rat smooth muscle cells (rSMCs) were cultured in a cell medium consisting of Dulbecco's modified Eagle's medium with 10% heat-inactivated fetal bovine serum and 1% penicillin/streptomycin at 37 °C and 5% CO₂ in an incubator. The cells were seeded at 2.5×10^6 per 1 mL per well in 6-well plates and then kept in an incubator overnight to allow cell attachment to the surface. The cell medium was removed, and 7 mL of fresh cell medium was added. The PDMS-SB sample (7 mg) was placed into a sterilized transwell insert having a 40 μ m nylon mesh to contact with the cell medium indirectly. The PDMS-SB samples were washed with DPBS and 70% EtOH and then sterilized by UV for 10 min before use. The 6-well plate was kept at 37 °C and 5% CO₂. At 24 and 72 h time points, the transwell insert and cell medium were removed and then 100 μL of MTS solution (CellTiter 96 AQueous One Solution Cell Proliferation Assay, Promega Corp., WI) in 1 mL of cell medium was added to each well. The 6-well plate was kept in the incubator for 1 h, and then, the absorbance was recorded at 490 nm using a microplate reader (SpectraMax, Molecular Devices, San Jose, CA). Blank cell medium without PDMS-SB was used as a negative control, and 1 M acrylamide in cell medium was used as a positive control. At the time point of 72 h, images with the Live/Dead assay were taken by a fluorescence microscope (TE2000-E, Nikon,

Tokyo, Japan) after live/dead staining with a Promokine Live/Dead Cell Staining Kit.

Characterization of Microfabrication Performance and Processes. If the developed PDMS—SB hybrid is to be a replacement for commercial PDMS in typical micro-electro-mechanical systems and microfluidic device fabrications (Scheme 1B), it is important to characterize its performance in those processes compared to the standard preparation of commercial PDMS (Sylgard 184) with a 10:1 ratio of elastomer base to curing agent.

A spin curve was established for both the PDMS–SB-1 and PDMS–SB-2 as well as the PDMS control (PDMS-C, Sylgard 184) so that the thickness of the material can be reliably selected for membrane applications. ^{11,12} The material was dispensed onto Si wafer chips in a spin coater (Laurell Technologies, North Wales, PA) and spun at 500 rpm for 10 s to spread and then at the final spin speed for 30 s to reach the final thickness. The selected final spin speeds were on the range of 1000–3000 rpm. After curing, the membrane thickness was measured with a surface profiler (KLA-Tencor, Milpitas, CA) at multiple locations across the area to account for any nonuniformity.

In addition, the bonding performance is of interest. It is well established that commercial PDMS can be bonded to itself or to glass by O2 plasma treatment. This process is critically necessary for the soft lithography process to fabricate microchannel devices and prevent any leaks between the layers. 13 To test this, an experiment similar to that reported 14,15 was adopted. A 600 μ m thick mold was fabricated from SU-8 negative photoresist (MicroChem, Newton, MA) on a Si wafer, which featured a 3 mm diameter "blister" and an input port (Figure S1). The PDMS was cast over this mold and then cut away and bonded to pieces of unpatterned PDMS or a cleaned glass slide by O2 plasma treatment (Deiner Electronic, Ebhausen, Germany) at 0.25 mbar for 25 s. Thirty-three-gauge stainless steel tubing was inserted into the input port, sealed with epoxy, and connected to a regulated gas supply and the blister pressurized. The pressure from the regulator was increased gradually until the bond failed, and the corresponding pressure was recorded as a measure of the bond strength.

Sample Microchannel Fabrication. SU-8 negative photoresist was deposited onto an Si wafer with a thickness of 200 μ m and patterned into the shape of the microchannel shown in Figure S1. The design features a branching path where the smallest channel width is 200 μ m. PDMS-C control and PDMS-SB were cast over the resulting mold and then peeled away and bonded to cleaned glass slides via O₂ plasma to form the complete microchannel with a 200 μ m × 200 μ m square cross section at the smallest point. The inlet and outlet were opened with a biopsy punch, and PTFE tubing was inserted into the

Figure 2. (A) Thick section (upper) and thin membranes (lower) of PDMS and PDMS–SB transferred to a glass slide. Thick PDMS–SB has a slightly cloudy appearance. (B) Irreversible optical transparency changes of PDMS–SB hybrid membranes between the dried and wet states.

opening. Water and blood flowed through the microchannels via a syringe pump.

Gas Transfer Performance. The gas transfer performance of the material was also assessed. This is of interest for devices such as microfluidic artificial lungs, ¹⁴ where PDMS is the only barrier between the blood and gas supply. The group has already performed experiments involving this gas transfer, 15 so those experiments were adapted to isolate the material of the membrane as the only variable. A proof-of-concept microchannel device was fabricated with a 20 μ m membrane of either PDMS-C or PDMS-SB spread over a PMMA acrylic substrate with breathing holes to interface with open air. A 400 μm thick layer of commercial PDMS was cut in the shape of the channel to form a wall, and then, an acrylic top plate with input and output ports was placed over top. CO2 saturated water was supplied through the input port by a syringe pump (Harvard Apparatus, Holliston, MA) at 0.1 mL/min and flowed through the microchannel. The water was collected from the output port. The pH was measured with a pH meter (Horiba, Kyoto, Japan) before and after as a measure of how much CO₂ was transferred out of the water through the membrane during the flow.

Blood Flow Testing with PDMS-SB Microfluidic Channels. The blood compatibility of the microchannels was compared in a continuous blood flow test setting. Minimally anticoagulated fresh ovine blood (0.5–0.625 U heparin/mL blood) was continuously flowed (0.02 mL/min) through each the PDMS and PDMS-SB microchannels for ~1 h using a syringe pump. The outlet tubing of the devices was left open and positioned above a collection reservoir to allow blood to freely flow out of the device at an atmospheric outlet pressure. The devices were immersed in PBS warmed to 37 °C throughout testing. The perfusion pressure at each device inlet was monitored via a digital manometer (Dwyer Instruments Inc., Michigan City, IN) and recorded every 30 s. Device samples were collected following the experiment for subsequent scanning electron microscopy.

Statistical Analyses. Data are presented as mean \pm standard deviation (SD). Data were analyzed by one-way ANOVA followed by a post hoc Newman–Keuls test. Significant differences were considered to exist at p < 0.05.

RESULTS AND DISCUSSION

Synthesis of SB-Diallyl and Characteristics of PDMS–SB Hybrid Membranes. SB-diallyl was synthesized from diallylmethylamine and 1,3-propanesultone with over 70% average yields. The chemical structure of SB-diallyl characterized by 1 H NMR is shown in Figure 1 and confirms successful synthesis and purification. The SB-diallyl shows the peaks at 5.80–6.0 and 5.50–5.65 ppm from the protons of carbon double bonds (CH₂=CH)₂ as well as the typical peaks from SB groups, 2.0–2.15 (2H, CH₂CH₂SO₃), 2.75–2.85 (2H, CH₂SO₃), 2.85–2.95 (3H, CH₃N), 3.20–3.3 (2H, CH₂N), and 3.65–3.90 (4H, (CH₂)₂N) at the ppm.

PDMS-SB hybrid samples were fabricated by mixing the synthesized SB-diallyl and a commercial PDMS (Sylgard 184, vinyl-terminated PDMS) with the curing agent to produce PDMS-SB hybrid membranes or microfluidic devices. A representative picture of the prepared PDMS and PDMS-SB hybrid membranes in both thick section (upper) and thin membrane (lower, outlined in the dashed line) form are shown in Figure 2A. Although a thick PDMS-SB sample has a slightly cloudy appearance, a thin PDMS-SB-1 membrane prepared by spin coating exhibited good optical transparency similar to the PDMS control. The PDMS-SB-2, hybrid samples with an increased SB-diallyl blending ratio, had increased opacity. However, under wet conditions, the material became transparent in an irreversible manner. The PDMS-SB-2 hybrid membranes showed good optical transparency after immersion in DI water (wet) (Figure 2B).

Mechanical properties of the fabricated samples characterized by uniaxial testing are shown in Table 1. The initial

Table 1. SB-Diallyl Mixing Ratio and the Mechanical Properties of PDMS-SB Hybrid Membranes

| | SB-diallyl mixing ratio (wt %) | initial modulus (MPa) | tensile strength (MPa) | breaking strain (%) | | |
|---|--------------------------------------|-----------------------------|------------------------------|------------------------|--|--|
| PDMS-C | 0 | 1.2 (±0.4) | 4.5 (±1.3) | 167 (±27) | | |
| PDMS-SB-1 | 0.5 | 1.4 (±0.2) | 4.1 (±0.4) | 149 (±19) | | |
| PDMS-SB-2 | 1.0 | 1.7 (±0.1) | 4.7 (±1.1) | $123 \ (\pm 12)^a$ | | |
| PDMS-SB-3 | 2.0 | 1.6 (±0.2) | $3.6 \ (\pm 0.4)$ | $112 \ (\pm 13)^a$ | | |
| ^{a}p < 0.05 vs PDMS-C and PDMS-SB-1, $n = 5$. | | | | | | |

modulus and ultimate tensile strength of PDMS–SB hybrids (PDMS–SB-1, PDMS–SB-2, and PDMS–SB-3) did not show significant differences compared to those of PDMS-C, while the breaking strains of PDMS–SB-2 and PDMS–SB-3 were decreased compared to those of the PDMS-C and PDMS–SB-1 (p < 0.05, n = 5). However, the mechanical properties of PDMS–SB hybrid could be varied and simply adjusted by controlling the mixing ratio of SB-diallyl, the amount of the curing agent as well as the curing temperature, similar to conventional PDMS processing. 12

Blood Biocompatibility of PDMS-SB Hybrid. Platelet deposition onto PDMS samples after fresh ovine blood contact for 2 h is shown in Figures 3 and S2. The commercial PDMS control (PDMS-C, Sylgard 184) surfaces showed relatively high levels of platelet deposition in organized thrombi with activated platelet aggregates as evidenced by pseudopodia extension and spreading (Figure 3A). Platelet deposition and

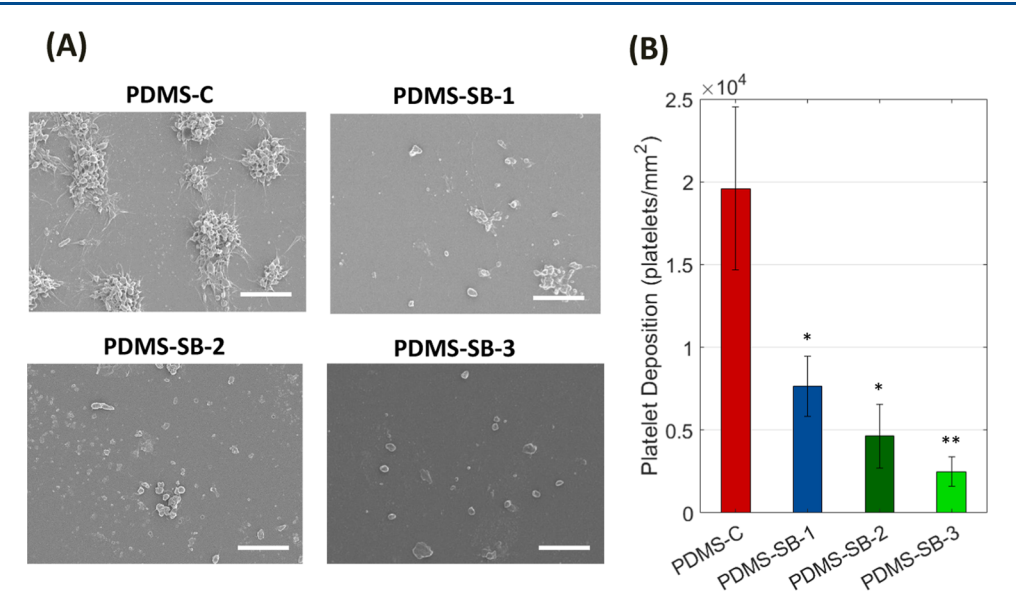


Figure 3. (A) Scanning electron micrographs of the PDMS control (PDMS-C and PDMS-SB hybrid surfaces) (scale bars = $10 \mu m$) and (B) platelet deposition quantified by lactate dehydrogenase (LDH) assay after contact with citrated ovine whole blood for 2 h at 37 °C (*p < 0.05 vs PDMS-C, **p < 0.05 vs PDMS and PDMS-SB-1, n = 5).

aggregate formation were remarkably reduced, and the deposited platelets were mostly in a resting morphology on PDMS–SB hybrid sample surfaces. The LDH results (Figure 3B) confirmed visual observations that the amount of platelet deposition on all PDMS–SB samples was markedly decreased compared with the PDMS control (p < 0.01, n = 5) and the amount of deposition was further decreased at higher SB content (p < 0.05, PDMS–SB-3 vs PDMS–SB-1).

The hemolytic index (% hemolysis) of the PDMS–SB hybrids demonstrated a nonhemolytic effect (since less than 2% compared to the negative control) and showed no significant difference compared to the PDMS control (p > 0.05, n = 3) (Figure S3). In addition, the cytotoxicity caused by contact with the elution medium of PDMS control and PDMS–SB hybrid samples showed no significant effect on rSMCs, with cell viability and growth in the elution media not affected vs the negative control, polymer contact-free cell medium (Figure S4).

Characterization of Microfabrication Performance and Processes. The spin curve generated for both the PMDS–SB-1 and PDMS–SB-2 is presented in Figure 4. From the data, it is seen that PDMS–SB-2 and PDMS–SB-1 are thinner than PDMS-C (p < 0.05). This is seen as neither an advantage nor a disadvantage, however, since the desired thickness can be chosen as long as the spin curve is known.

The results of the bond strength testing are shown in Table 2. Each value represents the average of three trials. It is clear from these results and by visual inspection that bonding was achieved, so the O₂ plasma treatment remains an option for bonding with both concentrations of PDMS—SB compared to PDMS—C. In most cases, except for the bonding of PDMS—C to itself, the mechanism of failure was by a material break, rather than delamination of the bonded layers, indicating that the true bond strength may be stronger than the material itself and is not the limiting factor for bonding performance. Though this difference in failure mechanism is expected to have played a role in the somewhat high variability in the results of the test, the results clearly show the comparable performance in bond strength between both concentrations of the PDMS—SB and

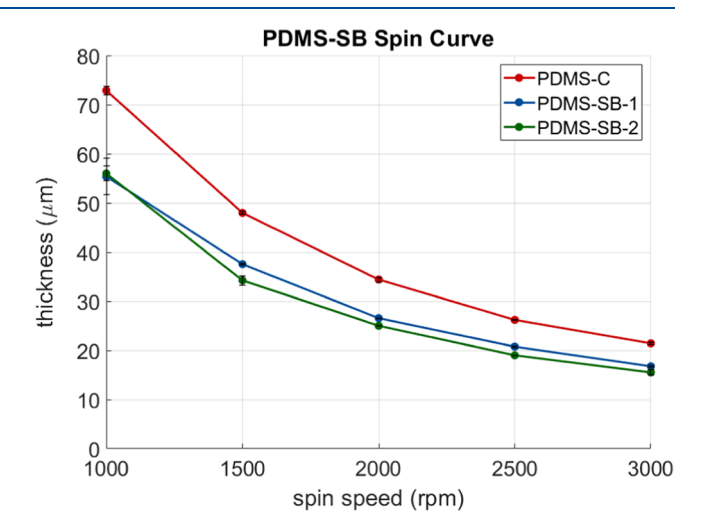


Figure 4. Spin curve for PDMS-SB hybrid membranes.

Table 2. Bond Strength (psi) of PDMS-SB Hybrid

| | | top material | |
|-----------------|-----------|--------------|-----------|
| bottom material | PDMS-C | PDMS-SB-1 | PDMS-SB-2 |
| glass | 68 (±7.0) | 61 (±5.5) | 67 (±7.0) |
| itself | 50 (±10) | 51 (±5.5) | 55 (±0.6) |

PDMS-C, indicating that the PDMS—SB should readily be able to replace the commercial PDMS in device fabrications involving bonding.

Gas Transfer Performance. The concentration of H⁺ calculated from the measured pH as an indicator of the transfer of CO₂ out of the microchannel flow through the PDMS membrane in the proof-of-concept gas transfer experiment is shown in Figure 5A. CO₂ saturated water was supplied at the inlet, and the differences of pH at the inlet and outlet were indicative of how much CO₂ was transferred out of water through the membrane during the flow. Each value represents the average of three trials. Both PDMS—SB hybrid membranes showed gas transfer out of the channel through the

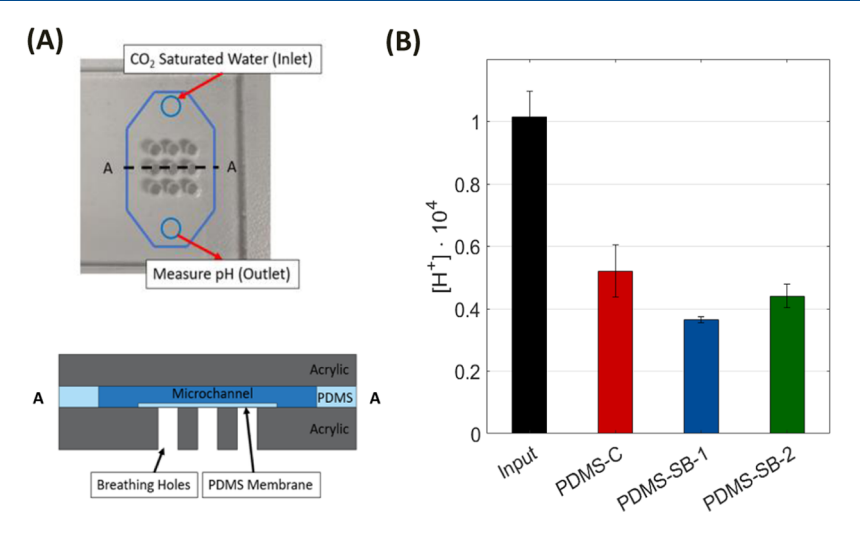


Figure 5. Top and side view schematic of the proof-of-concept on (A) a microfluidic artificial lung device and (B) the gas permeability of the PDMS-SB hybrid membrane and the control (Sylgard 184).

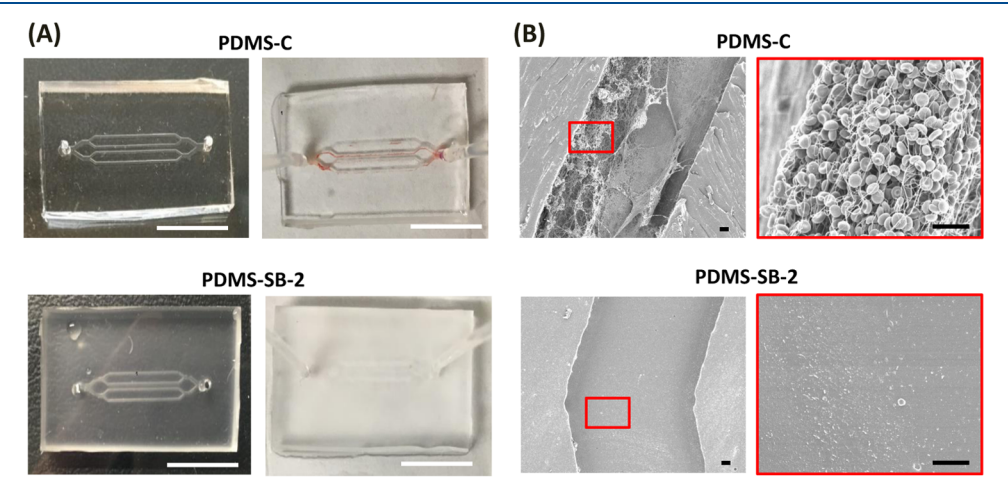


Figure 6. (A) Microchannel devices fabricated by PDMS and PDMS–SB hybrid polymers before and after contact with fresh ovine blood (flow rate = 0.02 mL/min) for 1 h (scale bars = 1 cm). (B) Scanning electron micrographs of the PDMS control and PDMS–SB hybrid microchannel after the blood contact (scale bars = $10 \mu m$).

membrane of comparable magnitude to the PDMS-C membrane (Figure 5B). While the results are not a conclusive measure of the gas permeability of the materials, they do show comparable performance of the PDMS-SB and commercial PDMS closer to an end application in this microfluidic artificial lung-type device, indicating that the PDMS-SB appears to perform comparably to commercial PDMS in this application.

Blood Flow Test with PDMS–SB Microfluidic Channels. Fabrication of the simplified microfluidic channel was also successful. The PDMS–SB could be cast over the SU-8 microchannel mold and retain its shape when removed without damaging the material or the mold, exhibiting compatibility with the soft lithography process for microscale devices (Figure S1). After the pieces were bonded with O₂ plasma, both water and blood were able to flow through the channel via delivery from a syringe with good optical transparency in the wet state, as seen in Figure 6A.

The blood compatibility of the microfluidic channel was assessed using the setup shown in Figure S5, and the ability to resist thrombus formation was clearly different between the microfluidic channels of PDMS and the PDMS–SB-2 hybrid. The PDMS-C microfluidic channel became progressively more

occluded over 1 h by thrombi, which was clearly observed macroscopically as well as microscopically (Figure 6). Conversely, the microfluidic channel made from the PDMS—SB hybrid remained patent during the test, and thrombotic deposition in the microchannel was visually confirmed to be markedly lower compared to the PDMS-C after continuous blood contact. The inlet pressure change (Figure 7) of the blood flow pathway also supported these results. The inlet pressures of PDMS-C microfluidic channel increased with some peaks and valleys that were attributed to clogging and opening with thrombotic deposition in the microchannel. In contrast, the pressure for the PDMS—SB-2 microchannel was stable during the continuous ovine blood perfusion for 1 h.

The majority of efforts to improve the antifouling properties of PDMS have focused on surface modification strategies. ^{1,4} However, physical or simple surface treatments to improve hydrophilicity can be temporary. Covalent and bulk-phase approaches are preferable to make a relatively stable surface and provide long-term antifouling. Some previous efforts have sought a convenient or simple method for PDMS modification utilizing poly(ethylene glycol) (PEG) or carboxybetaine incorporating a terminal vinyl group. ^{16–19} Zhou et al. ¹⁸

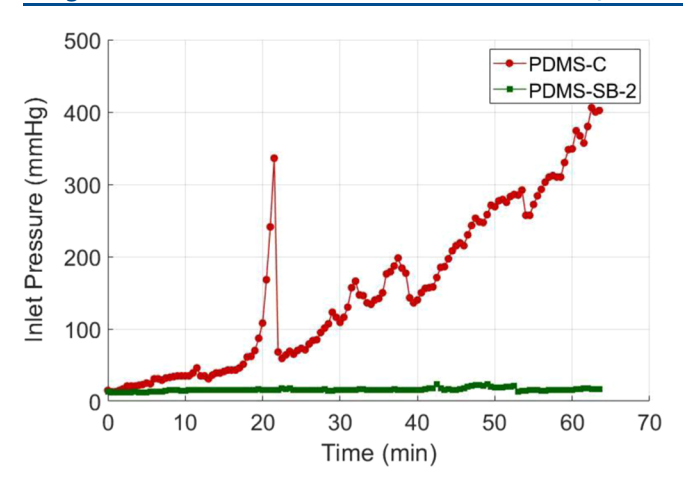


Figure 7. Pressure changes of the PDMS and PDMS–SB microchannel devices during a continuous blood contact test setting with fresh ovine blood (heparin 0.625 U/mL, flow rate = 0.02 mL/min).

demonstrated that a vinyl-functionalized PEG could be covalently linked to a PDMS network simultaneously when the PDMS is thermally cured. The results showed that small amounts of the PEG additive could greatly improve protein adsorption resistance since the conjugated PEG chains generated PEG nanodomains by phase separation from the PDMS domains. Zhang et al. 19 synthesized an allyl carboxybetaine to graft onto a Si-H functionalized PDMS, which was prepared by adjusting the molar ratio of the two components in Sylgard 184. The carboxybetaine-grafted PDMS films showed significantly improved blood biocompatibility with reduction of protein adsorption as well as bacteria adhesion. More recently, Gökaltun et al. 17 fabricated a hydrophilic PDMS microfluidic device by simple mixing with a PDMS-PEG block copolymer as an additive. They demonstrated that a small amount of PDMS-PEG blending (0.25 wt %) to a commercial PDMS could significantly reduce protein adsorption (up to 90%) and improve surface wettability with preserved mechanical and optical properties.

In this study, we synthesized a vinyl-terminated sulfobetaine (SB-diallyl) to integrate into a commercial PDMS (Sylgard 184) curing process. By direct and equivalent mixing of the SBdiallyl and Sylgard 184 base (vinyl-terminated PDMS) with the curing agent, SB moieties could be covalently bonded into the crosslinking PDMS chains (Figure 1B) simultaneously. Thus, this approach was considered an attractively simple way to fabricate an antifouling PDMS-SB hybrid membrane or microfluidic device using the conventional microfabrication process without additional steps for PDMS surface modification. Although the mechanical properties of PDMS-SB membranes were slightly altered with the amount of SB-diallyl introduced compared to those of the PDMS control, the mechanical properties could be controlled, with the initial modulus and breaking strain being tunable with the curing condition (data not shown). The PDMS-SB hybrid showed a decrease of optical transparency with the increased SB-diallyl additive, and the thicker samples were opaque. However, the optical transparency was improved with exposure to wet conditions and microfluidic channel visibility was not an issue. This interesting characteristic could be explained with the rearrangement of PDMS-SB molecular chains under dry and wet conditions¹⁷ since the hydrophilic SB groups might show some surface migration under an aqueous solution. As another

possible reason, swelling from the water absorption of the PDMS—SB sample might also affect the refraction of light to change the optical property. This swelling was measured and shown to be modest, however. Further detailed investigations would be necessary to clarify the reason. The fabricated PDMS—SB hybrid membranes showed a significant reduction of platelet deposition after fresh whole blood contact and were not hemolytic or cytotoxic to a primary vascular cell (rSMC). Importantly, the thickness of PDMS—SB membranes could be predictably adjusted with spin coating and showed a sufficient bonding strength between glass and the PDMS—SB itself. These characteristics allow the fabrication of a precise, thin membrane as well as designed micro/nano microfluidic devices using conventional microfabrication processes, as would be the case with commercial PDMS.

Since the synthesized SB-diallyl is a powder, HFIP was used as the solvent to mix it uniformly with the Sylgard 184 base and curing agent. Although other solvents (e.g., MeOH, water, 2-propanol) could also be used, the best results for PDMS—SB hybrid membrane formation were obtained when the HFIP solvent was used for SD-diallyl (Figure S6), since SB-diallyl could be dissolved in HFIP up to 50 wt % and mixed well with Sylgard 184 and the curing agent. Also, the HFIP solvent could be quickly evaporated during the mixing and air pocket elimination step under vacuum before moving to the curing process (at 60 °C for 4 h or at 90 °C for 1 h) since it is highly volatile. However, further refinement of the method may require improving miscibility or minimizing phase separation defects.

The stability of the SB molecules in the PDMS-SB hybrid and the long-term sustainability of the blood compatibility were also tested. To confirm the stability of SB moieties in the hybrid sample, a PDMS-SB-2 sample was soaked in PBS for 4 weeks at 37 °C (PDMS-SB-2 (4 weeks)), and the surface atomic composition was analyzed with energy-dispersive X-ray (EDX, Zeiss Sigma VP SEM, White Plains, NY) spectroscopy. The sulfur (S) atomic composition (%) from the SB moiety clearly appeared on both the PDMS-SB-2 (not soaked control) and PDMS-SB-2 (4 weeks) sample, and the % of S composition on PDMS-SB-2 (4 weeks) was similar with that of PDMS-SB-2 control (Table S1). The platelet deposition on the PDMS-SB-2 (4 weeks) sample after the ovine blood test (Figure S7) also indicated the stability of SB moieties and the sustainability of thromboresistance with the PDMS-SB hybrid. The amount of platelet deposition on PDMS-SB-2 (4 weeks) was similar to the PDMS-SB surfaces, which were not soaked in PBS for 4 weeks at 37 °C (Figure 3).

The water contact angles of PDMS–SB-1, 106.3 (\pm 0.2), and PDMS–SB-2, 106.8 (\pm 0.3), were slightly decreased compared to the that of PDMS-C, 111.2 (\pm 1.0) (*p < 0.05). However, there was no significant difference between the PDMS–SB-1 and PDMS–SB-2 as well as for samples tested in dry or wet states (Table S2). The water absorption (%) of PDMS–SB-2 was 4.4 (\pm 0.8)%, which was higher than those of PDMS–SB-1 and PDMS-C. However, those differences were modest (less than 5%). This result is not surprising since the SB content is less than 1 wt % vs 0 wt % in PDMS-C. Further detailed evaluations may be necessary for higher SB content and with varying amounts of the curing agent. These would need to be characterized depending on the applications.

PDMS-SB-2 was selected for further use in microfluidic device fabrication since PDMS-SB-2 exhibited good optical properties in the wet condition together with a significant

reduction in platelet deposition. Although the platelet deposition results for the PDMS—SB-3 were similar or better than for PDMS—SB-2 (Figure 3), further studies would be necessary with PDMS—SB-3 to optimize other properties such as mechanical and optical.

There is a limitation on the current hybridization method to maximize the SB content in PDMS-SB to enhance blood compatibility. In this study, we prepared PDMS-SB hybrids with a limited mixing ratio of SB-diallyl/PDMS base (0.5:1, 1:1, or 2:1 molar ratio); however, it may be possible to increase the SB-diallyl amount to some maximum (e.g., 5:1 or 10:1 of the molar ratio). Further studies are necessary to find the optimal mixing ratio of SB-diallyl and the curing agent to obtain the proper properties to fit its application. The current study focuses on a simple blending method using a SB-diallyl functional molecule to modify a commercial PDMS and to adapt the conventional microfabrication process; however, other surface-focused modification routes are also possible to increase the SB moiety on the blood-contacting surface. For instance, a pre-PDMS hybrid could also be fabricated by blending with diallylmethylamine instead of SB-diallyl, and then, the SB groups could be generated after device fabrication by fluxing with 1,3-propanesultone to generate surface SB groups. Other simple surface-focused modifications would be possible using a Si-H functionalized PDMS and then an allyl functional SB monomer could be grafted to the surface via the hydrosilylation reaction using a Karstedit catalyst. 19 These noted postmodification methods might have an advantage to improve antifouling properties by increasing the SB moieties on the surface; however, this comes at the expense of additional processing steps after the device fabrication. The current approach has a clear advantage for scaled-up production for antifouling PDMS devices, and the benefit of a more complicated approach is not apparent at this point.

In this study, we demonstrated a simple method to produce PDMS-SB hybrid membranes as well as microfluidic devices using a common microfabrication process. Although a microfluidic artificial lung device (Figure 5A) is a first potential application using the developed PDMS-SB hybrid, application of the material to a traditional hollow fiber membrane oxygenator or an artificial lung device could also be considered. Development of blood-compatible materials or surface coatings to reduce thrombotic deposition on commercially available extra- and intracorporeal blood-contacting devices are extremely important for patients who face a higher risk of developing thromboembolic events (e.g., COVID-19 patients). 20-24 Using devices with surfaces composed of more blood-biocompatible (nonthrombogenic) materials could reduce the level of anticoagulation therapy required and reduce complications associated with thrombosis risk, as well as anticoagulation-related bleeding risk.²⁴ Other potential applications using PDMS-zwitterionic hybrid polymers may include blood-contacting microdevices, ²⁵ antifouling flexible and implantable biosensors, ²⁶ bioinspired vascular grafts, ²⁷ and other various devices including tissue chips and artificial organs, or antifouling marine coatings.28

CONCLUSIONS

A diallyl-terminated sulfobetaine molecule (SB-diallyl) was synthesized and directly integrated with a commercial PDMS base (Sylgard 184) to simply produce a PDMS—SB hybrid. In contact with whole blood, the PDMS—SB hybrid surface showed significantly decreased platelet deposition when

compared with the PDMS control while also not showing evidence of hemolysis or cytotoxicity. The PDMS-SB hybrid could be easily spin coated to a membrane thickness for film creation, and a spin curve was generated for the typical microfabrication processes. The hybrid material retained the ability to bond to itself or glass by O2 plasma treatment, and the bond strength was comparable to commercial PDMS, facilitating fabrication of PDMS-SB microfluidic devices. The fabricated PDMS-SB microchannel showed improved blood compatibility, avoiding the thrombotic occlusion experienced by the PDMS control device. A proof-of-concept gas transfer device showed that the PDMS-SB hybrid membrane could be used in gas transfer applications with a permeability comparable to commercial PDMS in this application. Because all tests showed comparable or improved performance and did not require any additional fabrication steps, the results indicate that the PDMS-SB hybrid should be able to replace commercial PDMS in microchannel and microfluidic artificial lung applications while providing the benefit of improved antifouling properties.

ASSOCIATED CONTENT

Supporting Information

The Supporting Information is available free of charge at https://pubs.acs.org/doi/10.1021/acs.langmuir.1c03375.

Design for sample microchannel fabrication, additional SEM pictures for the platelet deposition, results of the hemolysis and cytocompatibility test, a continuous blood contact test setting and additional pictures of the microchannel test results, microscopic observation of the PDMS—SB membranes prepared by a spin coating, and platelet deposition on the PDMS—SB-2 after 4 weeks soaking test; tables for surface atom composition, surface water contact angle, water absorption, and swelling ratio of PDMS control and PDMS—SB samples (PDF)

AUTHOR INFORMATION

Corresponding Authors

Sung Kwon Cho — Department of Mechanical Engineering & Materials Science, University of Pittsburgh, Pittsburgh, Pennsylvania 15261, United States; orcid.org/0000-0001-7283-8839; Email: skcho@pitt.edu

William R. Wagner — McGowan Institute for Regenerative Medicine, University of Pittsburgh, Pittsburgh, Pennsylvania 15219, United States; Department of Surgery and Department of Chemical and Petroleum Engineering, University of Pittsburgh, Pittsburgh, Pennsylvania 15213, United States; orcid.org/0000-0003-0082-8089; Email: wagnerwr@upmc.edu

Authors

Anthony Mercader – Department of Mechanical Engineering & Materials Science, University of Pittsburgh, Pittsburgh, Pennsylvania 15261, United States

Sang-Ho Ye — McGowan Institute for Regenerative Medicine, University of Pittsburgh, Pittsburgh, Pennsylvania 15219, United States; Department of Surgery, University of Pittsburgh, Pittsburgh, Pennsylvania 15213, United States Seungil Kim — McGowan Institute for Regenerative Medicine, University of Pittsburgh, Pittsburgh, Pennsylvania 15219, United States; Department of Surgery, University of Pittsburgh, Pittsburgh, Pennsylvania 15213, United States Ryan A. Orizondo — McGowan Institute for Regenerative Medicine, University of Pittsburgh, Pittsburgh, Pennsylvania 15219, United States; Department of Bioengineering and Department of Plastic Surgery, University of Pittsburgh, Pittsburgh, Pennsylvania 15213, United States

Complete contact information is available at: https://pubs.acs.org/10.1021/acs.langmuir.1c03375

Author Contributions

^VA.M. and S.-H.Y. equally contributed to this work and are cofirst authors.

Notes

The authors declare no competing financial interest.

ACKNOWLEDGMENTS

This research was supported by the NSF Engineering Research Center for Revolutionizing Metallic Biomaterials (ERC-RMB) (Award # 0812348, National Science Foundation) and National Institutes of Health (Award # 1R03EB023620-01). This work was also in part supported by the NSF projects (NSF ECCS-1637815 and 1951051). The authors would like to thank the Center for Biological Imaging (CBI) of the University of Pittsburgh for their kind assistance with the SEM images and also thank Joseph Hanks, Teri Horgan, and others in the MIRM animal facility at the University of Pittsburgh who provided the fresh ovine blood for this study.

REFERENCES

- (1) Zhang, H.; Chiao, M. Anti-Fouling Coatings of Poly-(Dimethylsiloxane) Devices for Biological and Biomedical Applications. *J. Med. Biol. Eng.* **2015**, *35*, 143–155.
- (2) Pasman, T.; Grijpma, D.; Stamatialis, D.; Poot, A. Flat and Microstructured Polymeric Membranes in Organs-on-Chips. *J. R. Soc. Interface* **2018**, *15*, No. 20180351.
- (3) Potrich, C.; Lunelli, L.; Cocuzza, M.; Marasso, S. L.; Pirri, C. F.; Pederzolli, C. Simple PDMS Microdevice for Biomedical Applications. *Talanta* **2019**, *193*, 44–50.
- (4) Gokaltun, A.; Yarmush, M. L.; Asatekin, A.; Usta, O. B. Recent Advances in Nonbiofouling PDMS Surface Modification Strategies Applicable to Microfluidic Technology. *Technology* **2017**, *05*, 1–12.
- (5) Ye, S.-H.; Johnson, C. A.; Woolley, J. R.; Murata, H.; Gamble, L. J.; Ishihara, K.; Wagner, W. R. Simple Surface Modification of a Titanium Alloy with Silanated Zwitterionic Phosphorylcholine or Sulfobetaine Modifiers to Reduce Thrombogenicity. *Colloids Surf., B* **2010**, *79*, 357–364.
- (6) Zhang, Y.; Liu, Y.; Ren, B.; Zhang, D.; Xie, S.; Chang, Y.; Yang, J.; Wu, J.; Xu, L.; Zheng, J. Fundamentals and Applications of Zwitterionic Antifouling Polymers. *J. Phys. D: Appl. Phys.* **2019**, *52*, No. 403001.
- (7) Ye, S.-H.; Arazawa, D. T.; Zhu, Y.; Shankarraman, V.; Malkin, A. D.; Kimmel, J. D.; Gamble, L. J.; Ishihara, K.; Federspiel, W. J.; Wagner, W. R. Hollow Fiber Membrane Modification with Functional Zwitterionic Macromolecules for Improved Thromboresistance in Artificial Lungs. *Langmuir* 2015, 31, 2463–2471.
- (8) Chen, Y.; Ye, S.-H.; Zhu, Y.; Gu, X.; Higuchi, S.; Wan, G.; Wagner, W. R. Covalently-Attached, Surface-Eroding Polymer Coatings on Magnesium Alloys for Corrosion Control and Temporally Varying Support of Cell Adhesion. *Adv. Mater. Interfaces* 2020, 7, No. 2000356.
- (9) Keefe, A. J.; Brault, N. D.; Jiang, S. Suppressing Surface Reconstruction of Superhydrophobic PDMS Using a Superhydrophilic Zwitterionic Polymer. *Biomacromolecules* **2012**, *13*, 1683–1687.

- (10) Kim, S.; Ye, S.; Adamo, A.; Orizondo, R. A.; Jo, J.; Cho, S. K.; Wagner, W. R. A Biostable, Anti-Fouling Zwitterionic Polyurethane-Urea Based on PDMS for Use in Blood-Contacting Medical Devices. *J. Mater. Chem. B* **2020**, *8*, 8305–8314.
- (11) Eddings, M. A.; Johnson, M. A.; Gale, B. K. Determining the Optimal PDMS-PDMS Bonding Technique for Microfluidic Devices. J. Micromech. Microeng. 2008, 18, No. 067001.
- (12) Schneider, F.; Draheim, J.; Kamberger, R.; Wallrabe, U. Process and Material Properties of Polydimethylsiloxane (PDMS) for Optical MEMS. Sens. Actuators, A 2009, 151, 95–99.
- (13) Bhattacharya, S.; Datta, A.; Berg, J. M.; Gangopadhyay, S. Studies on Surface Wettability of Poly(Dimethyl) Siloxane (PDMS) and Glass under Oxygen-Plasma Treatment and Correlation with Bond Strength. J. Microelectromech. Syst. 2005, 14, 590–597.
- (14) Potkay, J. A. The Promise of Microfluidic Artificial Lungs. *Lab Chip* **2014**, *14*, 4122–4138.
- (15) Geng, H.; Feng, J.; Cho, S. K. In Augmentation of Gas Exchange Using Oscillating Microbubble Array, IEEE 29th International Conference on Micro Electro Mechanical Systems (MEMS), 2016; pp 757–760
- (16) Zhang, Z.; Borenstein, J.; Guiney, L.; Miller, R.; Sukavaneshvar, S.; Loose, C. Polybetaine Modification of PDMS Microfluidic Devices to Resist Thrombus Formation in Whole Blood. *Lab Chip* **2013**, *13*, 1963–1968.
- (17) Gökaltun, A.; Kang, Y. B.; Yarmush, M. L.; Usta, O. B.; Asatekin, A. Simple Surface Modification of Poly(Dimethylsiloxane) via Surface Segregating Smart Polymers for Biomicrofluidics. *Sci. Rep.* **2019**, *9*, No. 7377.
- (18) Zhou, J.; Yan, H.; Ren, K.; Dai, W.; Wu, H. Convenient Method for Modifying Poly(Dimethylsiloxane) with Poly(Ethylene Glycol) in Microfluidics. *Anal. Chem.* **2009**, *81*, 6627–6632.
- (19) Zhang, A.; Cheng, L.; Hong, S.; Yang, C.; Lin, Y. Preparation of Anti-Fouling Silicone Elastomers by Covalent Immobilization of Carboxybetaine. *RSC Adv.* **2015**, *5*, 88456–88463.
- (20) DeLaney, E.; Smith, M. J.; Harvey, B. T.; Pelletier, K. J.; Aquino, M. P.; Stone, J. M.; Jean-Baptiste, G. C.; Johnson, J. H. Extracorporeal Life Support for Pandemic Influenza: The Role of Extracorporeal Membrane Oxygenation in Pandemic Management. J. Extra Corpor. Technol. 2010, 42, 268–280.
- (21) Guo, Z.; Sun, L.; Li, B.; Tian, R.; Zhang, X.; Zhang, Z.; Clifford, S. P.; Liu, Y.; Huang, J.; Li, X. Anticoagulation Management in Severe Coronavirus Disease 2019 Patients on Extracorporeal Membrane Oxygenation. *J. Cardiothorac. Vasc. Anesth.* **2021**, *35*, 389–397.
- (22) Bemtgen, X.; Zotzmann, V.; Benk, C.; Rilinger, J.; Steiner, K.; Asmussen, A.; Bode, C.; Wengenmayer, T.; Maier, S.; Staudacher, D. L. Thrombotic Circuit Complications during Venovenous Extracorporeal Membrane Oxygenation in COVID-19. *J. Thromb. Thrombolysis* 2021, *51*, 301–307.
- (23) Hajra, A.; Mathai, S. V.; Ball, S.; Bandyopadhyay, D.; Veyseh, M.; Chakraborty, S.; Lavie, C. J.; Aronow, W. S. Management of Thrombotic Complications in COVID-19: An Update. *Drugs* **2020**, *80*, 1553–1562.
- (24) Merrill, J. T.; Erkan, D.; Winakur, J.; James, J. A. Emerging Evidence of a COVID-19 Thrombotic Syndrome Has Treatment Implications. *Nat. Rev. Rheumatol.* **2020**, *16*, 581–589.
- (25) Jain, A.; Graveline, A.; Waterhouse, A.; Vernet, A.; Flaumenhaft, R.; Ingber, D. E. A Shear Gradient-Activated Microfluidic Device for Automated Monitoring of Whole Blood Haemostasis and Platelet Function. *Nat. Commun.* **2016**, *7*, No. 10176.
- (26) Howe, C.; Mishra, S.; Kim, Y.-S.; Chen, Y.; Ye, S.-H.; Wagner, W. R.; Jeong, J.-W.; Byun, H.-S.; Kim, J.-H.; Chun, Y.; Yeo, W.-H. Stretchable, Implantable, Nanostructured Flow-Diverter System for Quantification of Intra-Aneurysmal Hemodynamics. *ACS Nano* **2018**, 12, 8706–8716.
- (27) Pocivavsek, L.; Ye, S.-H.; Pugar, J.; Tzeng, E.; Cerda, E.; Velankar, S.; Wagner, W. R. Active Wrinkles to Drive Self-Cleaning: A Strategy for Anti-Thrombotic Surfaces for Vascular Grafts. *Biomaterials* **2019**, *192*, 226–234.

(28) Rahimi, A.; Stafslien, S. J.; Vanderwal, L.; Finlay, J. A.; Clare, A. S.; Webster, D. C. Amphiphilic Zwitterionic-PDMS-Based Surface-Modifying Additives to Tune Fouling-Release of Siloxane-Polyurethane Marine Coatings. *Prog. Org. Coat.* **2020**, *149*, No. 105931.

TRecommended by ACS

Multifunctional Surface Modification of PDMS for Antibacterial Contact Killing and Drug-Delivery of Polar, Nonpolar, and Amphiphilic Drugs

Annija Stepulane, Martin Andersson, et al.

NOVEMBER 02, 2022 ACS APPLIED BIO MATERIALS

READ 🗹

PDMS-PEG Block Copolymer and Pretreatment for Arresting Drug Absorption in Microphysiological Devices

Devin B. Mair, Deok-Ho Kim, et al.

AUGUST 19, 2022

ACS APPLIED MATERIALS & INTERFACES

READ 🗹

Tough Hydrogel Coating on Silicone Rubber with Improved Antifouling and Antibacterial Properties

Lei Cheng, Xinsong Li, et al.

MARCH 31, 2022

ACS APPLIED POLYMER MATERIALS

READ 🗹

Nanoscaled Morphology and Mechanical Properties of a Biomimetic Polymer Surface on a Silicone Hydrogel Contact Lens

Xinfeng Shi, James Yuliang Wu, et al.

NOVEMBER 17, 2021

LANGMUIR

READ 🗹

Get More Suggestions >